JACS ARTICLES

Published on Web 11/10/2010

# Ligand Exchange Reactions on $Au_{38}$ and $Au_{40}$ Clusters: A Combined Circular Dichroism and Mass Spectrometry Study

Stefan Knoppe,[†] Asantha C. Dharmaratne,[‡] Ella Schreiner,[†] Amala Dass,*[,‡] and Thomas Bürgi*[,†]

*Physikalisch-Chemisches Institut, Universität Heidelberg, Im Neuenheimer Feld 253, D-69120 Heidelberg, Germany, and Department of Chemistry and Biochemistry, University of Mississippi, University, Mississippi 38677, United States*

Received May 28, 2010; E-mail: amal@olemiss.edu; buergi@uni-heidelberg.de

***Abstract:*** The thiolate-for-thiolate ligand exchange reaction between the stable $Au_{38}(2\text{-PET})_{24}$ and $Au_{40}(2\text{-PET})_{24}$ (2-PET: 2-phenylethanethiol) clusters and enantiopure BINAS (BINAS: 1,1′-binaphthyl-2,2′-dithiol) was investigated by circular dichroism (CD) spectroscopy in the UV/vis and MALDI mass spectrometry (MS). The ligand exchange reaction is incomplete, although a strong optical activity is induced to the resulting clusters. The clusters are found to be relatively stable, in contrast to similar reactions on $[Au_{25}(2\text{-PET})_{18}]^-$ clusters. Maximum anisotropy factors of $6.6 \times 10^{-4}$ are found after 150 h of reaction time. During the reaction, a varying ratio between $Au_{38}$ and $Au_{40}$ clusters is found, which significantly differs from the starting material. As compared to $Au_{38}$, $Au_{40}$ is more favorable to incorporate BINAS into its ligand shell. After 150 h of reaction time, an average of 1.5 and 4.5 BINAS ligands is found for $Au_{38}$ and $Au_{40}$ clusters, respectively. This corresponds to exchange of 3 and 9 monodentate 2-PET ligands. To show that the limited exchange with BINAS is due to the bidentate nature of the ligand, exchange with thiophenol was performed. The monodentate thiophenol exchange was found to be faster, and more ligands were exchanged when compared to BINAS.

## Introduction

Noble metal nanoparticles and nanoclusters are a vibrant field in modern research.[1,2] Ultrasmall thiolate-protected gold clusters (<2 nm) have been widely studied since 1994, when Brust and Schiffrin presented a phase transfer agent-mediated two-phase synthesis.[3−5] The clusters produced in this approach and related syntheses are polydisperse. Monodisperse clusters are obtained from size separation processes such as solvent fractionation, gel electrophoresis, or size exclusion chromatography.[5−8] Recently, synthetic approaches to highly monodisperse $Au_n(SR)_m$ clusters such as $n = 25$, 38 ($m = 18$, 24) were reported.[9−13] Monodisperse clusters show quantum confinement effects, for example, defined UV/vis profiles with characteristic signatures. Besides fundamental interests, possible applications lie in the fields of catalysis, biosensors, and material sciences.[1,14,15]

The recently solved crystal structures of $Au_{102}(p\text{-MBA})_{44}$ (*p*-MBA: *para*-mercapto benzoic acid) and $[Au_{25}(2\text{-PET})_{18}]^-$ have aroused significant interest.[10,16,17] Structural aspects and comparison to phosphine stabilized clusters led to the formulation of a superatom complex model that explains formulas and charge of gold clusters.[18] In this model, spherical clusters with shell-closing electron counts $n^* = 2$, 8, 18, 34, 58, ... are associated with extraordinary stability. $[Au_{25}(2\text{-PET})_{18}]^-$ and $Au_{102}(p\text{-MBA})_{44}$ herein correspond to $n^* = 8$ and 58, respectively. Other identified stable species such as $Au_{68}(SR)_{34}$ ($n^* = 34$) confirm this model.[19]

[†] Universität Heidelberg.
[‡] University of Mississippi.

(1) Daniel, M.-C.; Astruc, D. *Chem. Rev.* **2004**, *104*, 293–346.
(2) Sardar, R.; Funston, A. M.; Mulvaney, P.; Murray, R. W. *Langmuir* **2009**, *25*, 13840–13851.
(3) Brust, M.; Walker, M.; Bethel, D.; Schiffrin, D. J.; Whyman, R. *J. Chem. Soc., Chem. Commun.* **1994**, 801–802.
(4) Price, R. C.; Whetten, R. L. *J. Am. Chem. Soc.* **2005**, *127*, 13750–13751.
(5) Whetten, R. L.; Khoury, J. T.; Alvarez, M. M.; Murthy, S.; Vezmar, I.; Wang, Z. L.; Stephens, P. W.; Cleveland, C. L.; Luedtke, W. D.; Landman, U. *Adv. Mater.* **1996**, *8*, 428–433.
(6) Chaki, N. K.; Negishi, Y.; Tsunoyama, H.; Shichibu, Y.; Tsukuda, T. *J. Am. Chem. Soc.* **2008**, *130*, 8608–8610.
(7) Schaaff, T. G.; Whetten, R. L. *J. Phys. Chem. B* **2000**, *104*, 2630–2641.
(8) Gautier, C.; Taras, R.; Gladiali, S.; Bürgi, T. *Chirality* **2008**, *20*, 486–493.
(9) (a) Donkers, R. L.; Lee, D.; Murray, R. W. *Langmuir* **2004**, *20*, 1945–1952. (b) Donkers, R. L.; Lee, D.; Murray, R. W. *Langmuir* **2008**, *24*, 5976–5976.
(10) Heaven, M. W.; Dass, A.; White, P. S.; Holt, K. M.; Murray, R. W. *J. Am. Chem. Soc.* **2008**, *130*, 3754–3755.
(11) Whu, Z.; Suhan, J.; Jin, R. *J. Mater. Chem.* **2009**, *19*, 622–626.
(12) Qian, H.; Zhu, M.; Andersen, U. N.; Jin, R. *J. Phys. Chem. A* **2009**, *113*, 4281–4284.
(13) Tokkainen, O.; Ruiz, V.; Rönnholm, G.; Kalkinnen, N.; Liljeroth, P.; Quinn, B. M. *J. Am. Chem. Soc.* **2008**, *130*, 11049–11055.
(14) Ghosh, S.; Kundu, K. S.; Mandal, M.; Pal, T. *Langmuir* **2002**, *18*, 8756–8760.
(15) Elghanian, R.; Storhoff, J. J.; Mucic, R. C.; Letsinger, R. L.; Mirkin, C. A. *Science* **1997**, *277*, 1078–1081.
(16) Jadzinsky, P. D.; Calero, G.; Ackerson, C. J.; Bushnell, D. A.; Kornberg, R. D. *Science* **2007**, *318*, 430–433.
(17) Whetten, R. L.; Price, R. C. *Science* **2007**, *318*, 407–408.
(18) Walter, M.; Akola, J.; Lopez-Acevedo, O.; Jadzinsky, P. D.; Calero, G.; Ackerson, C. J.; Whetten, R. L.; Grönbeck, H.; Häkkinen, H. *Proc. Natl. Acad. Sci. U.S.A.* **2008**, *105*, 9157–9162.
(19) Dass, A. *J. Am. Chem. Soc.* **2009**, *131*, 11666–11667.

  

Mass spectrometry has been established as a powerful tool in the characterization of gold nanoclusters. ESI and MALDI-TOF mass spectrometry (MS) have been used to identify even the nature of the protecting layers.[20−22] MALDI-TOF MS is suitable for direct assignment of nanocluster formula by obtaining intact, nonfragmented cluster ions and also facilitates the analysis of mixtures of nanoparticles.[19,23]

The chiroptical effects have extensively been studied recently, after Schaaff and Whetten observed optical activity for glutathione thiolate (GS) stabilized $Au_{25}$ clusters (albeit originally assigned as $Au_{38}$ or $Au_{28}$).[24−27] Electronic and vibrational circular dichroism spectroscopy were used to investigate these properties and to perform conformational analyses of the protecting chiral ligands in the clusters, backed by computational studies.[26] Similar studies were conducted for silver and palladium nanoclusters and phosphine-stabilized gold nanoclusters.[28−30] The induced optical activity increases with the number of anchoring points to the ligand. The largest maximum anisotropy factors $\Delta A/A$ ($4 \times 10^{-3}$) were found for $Au_{11}(BINAS)_m$ clusters.[8]

Ligand exchange reactions on chiral gold nanoclusters have been studied recently.[31,32] In the case of *N*-isobutyryl-cysteine protected $Au_n$ clusters ($n = 15, 18$), the core size is found to be conserved upon exchange with different thiol ligands. In similar studies on $[Au_{25}(2\text{-PET})_{18}]^-$ clusters, the size is not conserved upon exchange with BINAS, although optically active species are formed. Yao described an increase of optical activity in racemic penicillamine protected silver clusters upon treatment with enantiopure penicillamine.[33] Detailed kinetic studies of thiolate-for-thiolate exchange reactions have been performed by Pradeep and Murray.[34,35]

The etching method to prepare nanoclusters from other nanoclusters of higher mass has been introduced by Schaaff and Whetten in 1999.[36] They also observed the formation of a white-yellow insoluble material, assigned as Au(I)-S-polymers. Recent efforts by several groups resulted in the identification of $Au_{38}(SR)_{24}$ and $Au_{144}(SR)_{60}$.[6,37,38] $Au_{38}(SR)_{24}$ clusters have been synthesized by Quinn and co-workers by treatment of polydisperse clusters in excess thiol and in high yield by Jin and co-workers by thermal etching of glutathione thiolate (GS) protected $Au_n$ clusters ($n = 40-102$).[12,13,39] Very recently, $Au_{40}(SR)_{24}$ was characterized as an intermediate and byproduct in this process.[40] The thermal etching process employed in the $Au_{38}$ synthesis is a two-phase reaction that undergoes replacement of all the ligands. Similar reactions, such as the synthesis of $[Au_{25}(SG)_{18}]^-$ from $Au_n(PPh_3)_m$ clusters ($PPh_3$: triphenylphosphine), have been reported before.[41]

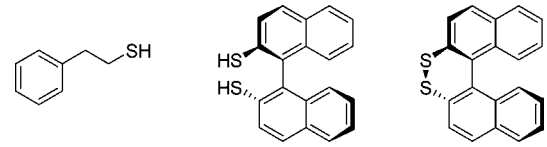


***Figure 1.*** Structures of 2-phenylethanethiol (2-PET) (left), *S*-1,1′-binaphthyl-2,2′dithiol (*S*-BINAS) (middle), and its cyclic disulfide (right).

Herein, we report on the ligand exchange reaction of achiral $Au_{38}(2\text{-PET})_{24}$ with a chiral dithiol, BINAS (Figure 1). For comparison, exchange with monodentate thiophenol was performed. The reaction was monitored by both circular dichroism spectroscopy (CD) and MALDI MS up to 150 h. CD spectroscopy provides information about the chiroptical properties of the samples, but does not provide information about the number of exchanged ligands. Mass spectrometry, on the other hand, cannot discriminate between chiral species, but gives insight into the molecular composition of intact clusters and offers a quantitative analysis of the reaction products.[22,23] To the best of our knowledge, the dependence of optical activity on the number of chiral ligands by combining MS and CD spectroscopy has not yet been reported for chiral gold nanoclusters.

## Experimental Section

**Materials.** L-Glutathione reduced (Sigma-Aldrich, >99%), sodium borohydride (Aldrich, 98.5%), acetone (Fisher, 99.7%), toluene (Fisher, 99.9%), ethanol (Sigma-Aldrich, >99.8%), methanol (Fisher, 99.9%), 2-phenylethanethiol (Aldrich, 99+%), thiophenol (Sigma-Aldrich, >99%), dichloromethane (Merck, 99.7+%), and 3-(4-*tert*-butylphenyl)-2-methyl-2-propenylidene]malononitrile (Fluka, >99.0%) were used as received. Nanopure water (≥18 MΩ) was used. $HAuCl_4$ was prepared by literature methods.[42] Enantiopure BINAS was synthesized after De Lucchi's protocol.[43]

**Synthesis of $Au_{38}(2\text{-PET})_{24}$/$Au_{40}(2\text{-PET})_{24}$.** $HAuCl_4$ (1 g, 2.54 mmol) and glutathione (3.1 g, 10.18 mmol) were dissolved in 200 mL of methanol and 100 mL of distilled water, respectively, at room temperature, and the solutions were mixed and vigorously stirred for 15 min at 0 °C. A light brown/white cloudy suspension was formed. A solution of $NaBH_4$ (1.1 g, 30 mmol, in 60 mL of $H_2O$) was added, resulting in a dark brown/black suspension and stirred for 1 h. The black nanoclusters were collected by centrifugation and further washed with methanol.

$Au_n(SG)_m$ nanoclusters (from step 1) were dissolved in 10 mL of distilled water in a 50 mL round-bottomed flask. Subsequently, 10 mL of acetone and 15 mL of 2-phenylethanethiol were added, and the solution was stirred at 80 °C for 3 h. Next, the phases were separated. Thirty milliliters of methanol and 1 mL of water were added to the organic phase. The black precipitate was washed with methanol (three times) to remove excess thiol. $Au_{38}/Au_{40}$

(20) Tracy, J. B.; Kalyuzhny, G.; Crowe, M. C.; Balasubramanian, R.; Choi, J.-P.; Murray, R. W. *J. Am. Chem. Soc.* **2007**, *129*, 6706–6707.
(21) Tracy, J. B.; Crowe, M. C.; Parker, J. F.; Hampe, O.; Fields-Zinna, C. A.; Dass, A.; Murray, R. W. *J. Am. Chem. Soc.* **2007**, *129*, 16209–16215.
(22) Dass, A.; Stevenson, A.; Dubay, G. R.; Tracy, J. B.; Murray, R. W. *J. Am. Chem. Soc.* **2008**, *130*, 5940–5946.
(23) Dharmaratne, A. C.; Krick, T.; Dass, A. *J. Am. Chem. Soc.* **2009**, *131*, 13604–13605.
(24) Gautier, C.; Bürgi, T. *ChemPhysChem* **2009**, *10*, 483–492.
(25) Schaaff, T. G.; Knight, G.; Shafigullin, M. N.; Borkman, R. F.; Whetten, R. L. *J. Phys. Chem. B* **1998**, *102*, 10643–10646.
(26) Gautier, C.; Bürgi, T. *Chem. Commun.* **2005**, *43*, 5393–5395.
(27) Yao, H.; Miki, K.; Nishida, N.; Sasaki, A.; Kimura, K. *J. Am. Chem. Soc.* **2005**, *127*, 15536–15543.
(28) Yao, H.; Nishida, N.; Kimura, K. *Chem. Phys.* **2010**, *368*, 28–37.
(29) Tamura, M.; Fujihara, H. *J. Am. Chem. Soc.* **2003**, *125*, 15742–15743.
(30) Yanagimoto, Y.; Negishi, Y.; Fujihara, H.; Tsukuda, T. *J. Phys. Chem. B* **2006**, *110*, 11611–11614.
(31) Gautier, C.; Bürgi, T. *J. Am. Chem. Soc.* **2008**, *130*, 7077–7084.
(32) Si, S.; Gautier, C.; Boudon, J.; Taras, R.; Gladiali, S.; Bürgi, T. *J. Phys. Chem. C* **2009**, *113*, 12966–12969.
(33) Nishida, N.; Yao, H.; Kimura, K. *Langmuir* **2008**, *24*, 2759–2766.
(34) Shibu, E. S.; Habeeb Muhammed, M. A.; Tsukuda, T.; Pradeep, T. *J. Phys. Chem. C* **2008**, *112*, 12168–12176.
(35) Dass, A.; Holt, K.; Parker, J. F.; Feldberg, S. W.; Murray, R. W. *J. Phys. Chem. C* **2008**, *112*, 20276–20283.
(36) Schaaff, T. G.; Whetten, R. L. *J. Phys. Chem. B* **1999**, *103*, 9394–9396.
(37) Qian, H.; Jin, R. *Nano Lett.* **2009**, *9*, 4083–4087.
(38) Fields-Zinna, C. A.; Sardar, R.; Beasley, C. J.; Murray, R. W. *J. Am. Chem. Soc.* **2009**, *131*, 16266–16271.
(39) Qian, H.; Zhu, Y.; Jin, R. *ACS Nano* **2009**, *3*, 3795–3803.
(40) Qian, H.; Zhu, Y.; Jin, R. *J. Am. Chem. Soc.* **2010**, *132*, 4583–4585.
(41) Shishibu, Y.; Negishi, Y.; Tsukuda, T.; Teranishi, T. *J. Am. Chem. Soc.* **2005**, *127*, 13464–13465.
(42) Brauer, G. *Handbook of Preparative Inorganic Chemistry*; Academic Press: New York, 1965.
(43) Fabbri, D.; Delogu, G.; De Lucchi, O. *J. Org. Chem.* **1993**, *58*, 1748–1750.

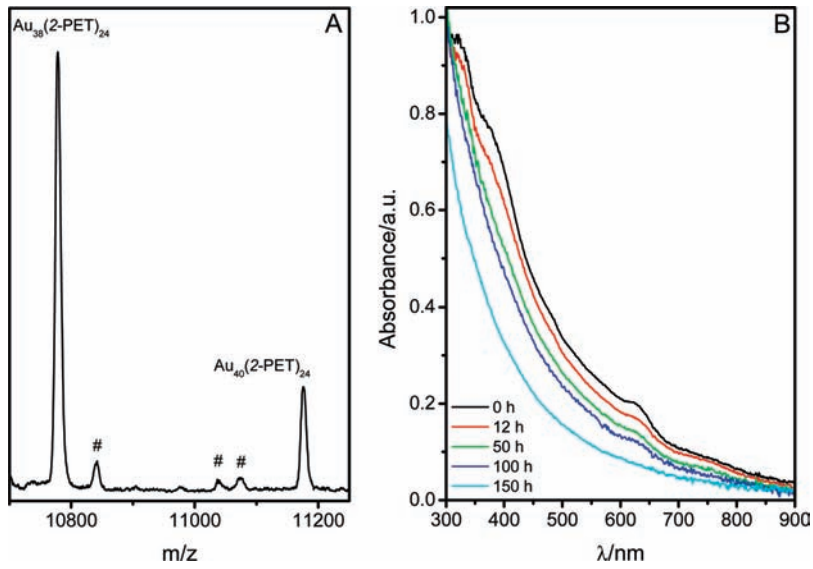


***Figure 2.*** (A) MALDI mass spectrum of the starting material, containing $Au_{38}$, $Au_{38}(2\text{-PET})_{24}$, and minor quantities of $Au_{40}$, $Au_{40}(2\text{-PET})_{24}$, using DCTB matrix. The signals assigned with # are fragments (see the Supporting Information); (B) UV/vis spectra of $Au_{38}(2\text{-PET})_{24}$ before and after exchange with BINAS at different reaction times. The spectra were normalized to an absorbance of 1 at 300 nm, except for 150 h.

nanoclusters were extracted with toluene. Methanol washing and toluene extraction was repeated to improve the purity of the product.

**Ligand Exchange between $Au_{38/40}(2\text{-PET})_{24}$ and BINAS.** For ligand exchange reactions, the clusters were dissolved in methylene chloride and treated with a huge molar excess of enantiopure BINAS (BINAS:$Au_{38}$ = 120:1, BINAS:2-PET = 5:1).

In a typical reaction, 3.6 mg of $Au_{38}(2\text{-PET})_{24}/Au_{40}(2\text{-PET})_{24}$ (88:12) was dissolved in 7.5 mL of methylene chloride and purged with argon. 12.8 mg of enantiopure BINAS was added, and the mixture was stirred at room temperature under argon. Aliquots (0.5−1 mL) were taken, and the solvent was removed in vacuo. The residual precipitates were washed with 12−15 mL of ethanol, redissolved in methylene chloride, concentrated, and again washed with ethanol. Overall, three washing cycles were applied for each sample.

**Ligand Exchange between $Au_{38/40}(2\text{-PET})_{24}$ and Thiophenol.** For ligand exchange reactions, the clusters were dissolved in methylene chloride and treated with a huge molar excess of thiophenol (thiophenol:$Au_{38}$ = 120:1, thiophenol:2-PET = 5:1).

In a typical reaction, 6.2 mg of $Au_{38}(2\text{-PET})_{24}/Au_{40}(2\text{-PET})_{24}$ (86:14) was dissolved in 12.4 mL of methylene chloride and purged with argon. Seven microliters of thiophenol was added, and the mixture was stirred at room temperature under argon. Aliquots (0.5−1 mL) were taken, and the solvent was removed in vacuo. The residual precipitates were washed with 12−15 mL of ethanol, redissolved in methylene chloride, concentrated, and again washed with ethanol. Overall, three washing cycles were applied for each sample.

**UV/Vis and CD Spectra.** For in situ studies, a sample of the reaction mixture was taken and diluted (ca. 1:3) to obtain a good CD signal. The sample was purged with argon and sealed in a quartz glass cuvette (path length 10 mm) equipped with a magnetic stirrer bar.

UV/vis spectra were measured on an AvaSpec 2048 UV/vis spectrophotometer. CD spectra were recorded on a JASCO J-715 CD spectrometer. CD spectra were obtained by averaging 12 scans with a scanning speed of 100 nm/min and a data pitch of 0.2 nm. For in situ measurements, 6 scans with a scanning speed of 200 nm/min were averaged to keep the acquisition time as short as possible. The signal of the bare solvent was subtracted from the CD signal of the sample. Anisotropy factors $g$ were obtained from division of the CD and UV spectra recorded at the same concentration ($g = \Theta/(32\,980*A)$). All spectra were recorded in methylene chloride.

**MALDI-TOF Analysis.** Mass spectra were obtained using a Bruker Autoflex mass spectrometer equipped with a nitrogen laser at near threshold laser fluence in positive linear mode. 3-(4-*tert*-Butylphenyl)-2-methyl-2-propenylidene]malononitrile (DCTB) was used as the matrix with 1:1000 analyte:matrix ratio. Two microliters of the analyte/matrix mixture was applied to the target and air-dried.

## Results and Discussion

**Starting Material.** $Au_{38}(2\text{-PET})_{24}$ was prepared by thermal etching of glutathionate stabilized $Au_n$ clusters by modification of earlier work.[12] The MALDI mass spectrum (Figure 2A) of the clusters exhibits a composition of 88% $Au_{38}(2\text{-PET})_{24}$ and 12% $Au_{40}(2\text{-PET})_{24}$. The later was unexpected and recently identified as a reaction byproduct in the etching process.[40] The $Au_{38}$ peak is found at $m/z$ = 10 778 (calculated: 10 778.08), and the $Au_{40}$ signal appears at $m/z$ = 11 174 (calculated: 11 172.02). Both signals therefore correspond to the unfragmented molecular ions. Spectra of ligand exchanged material were calibrated with the $Au_{38}$ peak at $m/z$ = 10 778.

**Ligand Exchange Reactions.** For ligand exchange, the starting material was dissolved in methylene chloride, and a 120-fold molar excess *R*- or *S*-BINAS (or thiophenol, respectively) was added. For the calculations, pure $Au_{38}$ was assumed. In five out of six runs, *S*-BINAS was used. The reaction mixture was stirred under argon atmosphere at room temperature. Samples were purified by washing with ethanol. Small amounts of a colorless material were observed, which dissolves neither in ethanol nor in methylene chloride. For in situ measurements, a sample of the reaction mixture was diluted by factor 3 to obtain an acceptable optical absorption and sealed in a UV/vis quartz glass cuvette equipped with a magnetic stirrer bar under argon atmosphere.

**UV/Vis Spectroscopy.** The UV/vis spectra of $Au_{38}$ clusters before and after ligand exchange both exhibit its characteristic signature with signals at 625 and 755 nm (less defined), as well as some characteristic shoulders at lower wavelengths, one of them at 370 nm (vide infra).[12] After 150 h of reaction time, the UV/vis profile becomes featureless, indicating partial decomposition of $Au_{38}$ clusters (but the MS shows $Au_{38}$ and $Au_{40}$ signals at 150 h, vide infra) (Figure 2B).

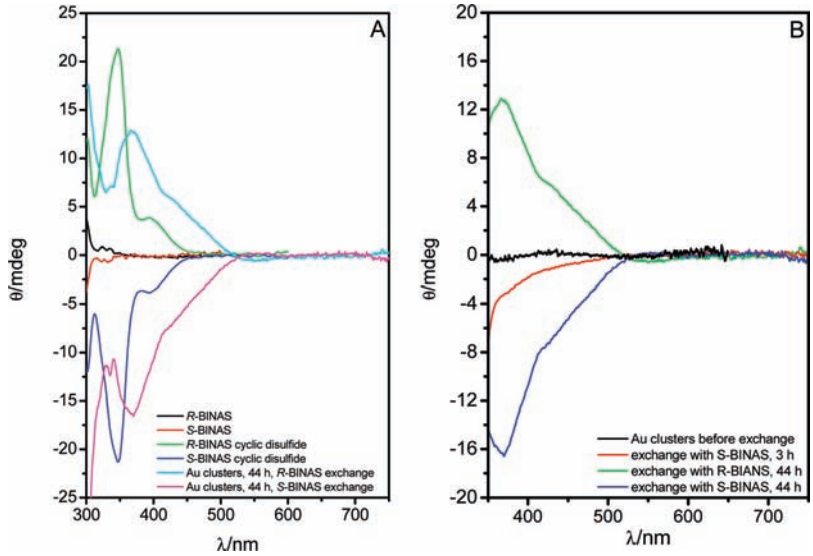


***Figure 3.*** (A) CD spectra of *R*- and *S*-BINAS and its cyclic disulfides as compared to ligand exchange products after 44 h; (B) CD spectra of ligand exchange products after 3 and 44 h (the 3 h sample is in situ).

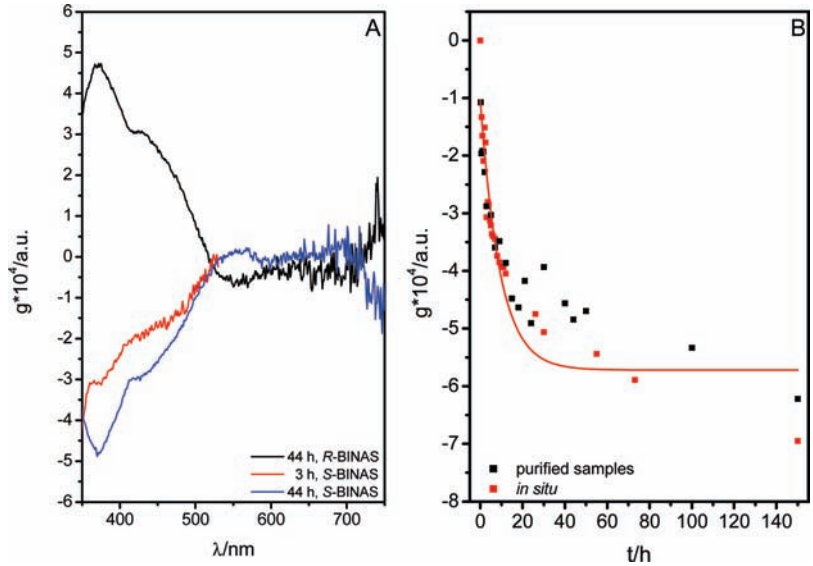


***Figure 4.*** (A) Anisotropy factors of ligand exchange products after 3 and 44 h (the 3 h sample is in situ); (B) anisotropy factors at 371 nm found for purified and in situ samples at different reaction times (exchange with *S*-BINAS). The black dots represent purified samples, as the red dots correspond to in situ measurements. Fit curve: exponential fit ($R^2 = 0.89717$).

**CD Spectroscopy.** After ligand exchange, significant optical activity is observed in the cluster samples (Figure 3). The optical activity increases with time, and a maximum at 370 nm as well as less intense signals at 555 and 625 nm and a shoulder at 410 nm are observed. The transition at 755 nm shows a rather strong anisotropy factor, although it is quite noisy (Figure 4A). The red shift as compared to free BINAS and its cyclic disulfide, which might occur in traces, is clear evidence for the transfer of optical activity on the electrons in the cluster, allowing the assumption of a successful ligand exchange, at least partial. Reaction with the two enantiomers of BINAS leads to perfect mirror images, indicating the formation of enantiomeric species.

As compared to a 3 h species (in situ), the optical activity increases after 44 h. This is even more evident in the anisotropy factors $g = \Delta A/A = \Delta\varepsilon/\varepsilon$, which are concentration independent. The maximum anisotropy factors after 44 h are ca. $5 \times 10^{-4}$, which is a typical value for gold nanoclusters.

In situ measurements were performed over the course of 150 h to obtain more information on the evolution of optical activity during the exchange reaction. Independent reactions were run to obtain purified samples for mass spectrometric analysis. Because a new signal at 371 nm evolves in the CD spectra, the anisotropy factors at 371 nm were studied as a function of time (Figure 4B). The values gained in situ strongly increase within the first hours of reaction time but begin to saturate after around 20 h. A notable optical activity is found within 15 min ($1.1 \times 10^{-4}$), and one-half of the anisotropy factor after 150 h (ca. $6.6 \times 10^{-4}$) is found after 6 h. The values for purified samples follow this curve with slightly smaller absolute values at longer times. The biggest difference was found to be $1 \times 10^{-4}$ after 30 h. Note that these values were gained from four different reaction batches.

Differences in concentration and temperature (fluctuations in room temperature) do not seem to affect the general profile of

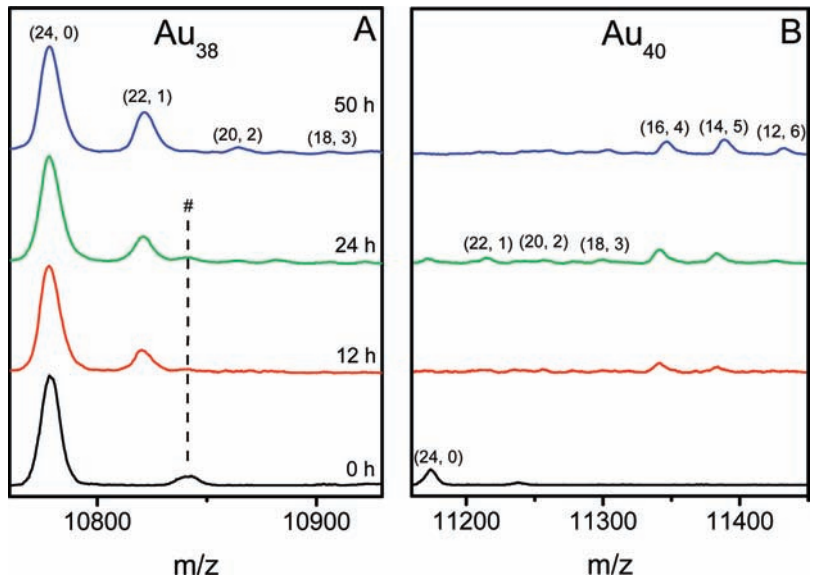


***Figure 5.*** (A) MALDI mass spectra of $Au_{38}$ signal set with time (0, 12, 24, 50 h) during ligand exchange with BINAS; (B) MALDI mass spectra of $Au_{40}$ signal set with time (0, 12, 24, 50 h) during ligand exchange with BINAS. The assignment of the signals is as follows: (*x*, *y*) corresponds to number of 2-PET and BINAS ligands. # denotes fragments.

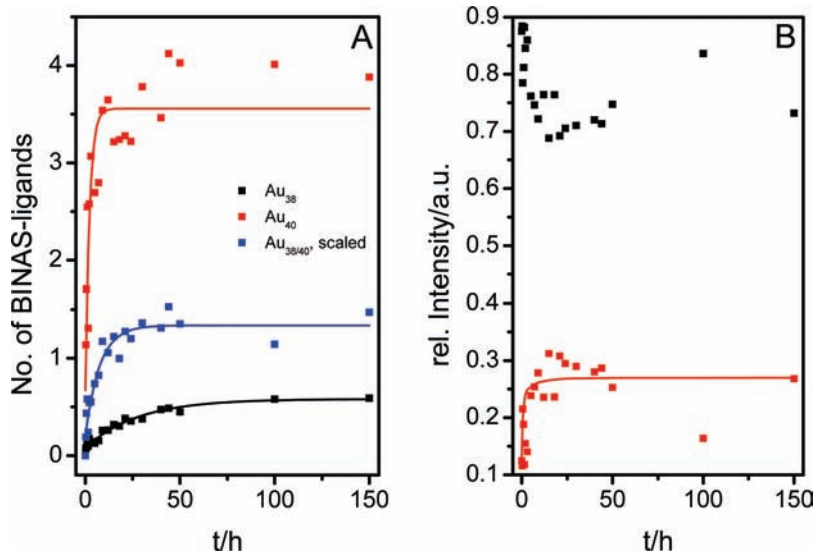


***Figure 6.*** (A) Number of BINAS ligands found for $Au_{38}$ and $Au_{40}$ clusters after reaction at different times; (B) relative abundances of $Au_{38}$ and $Au_{40}$ clusters with time. Color code: black, $Au_{38}$; red, $Au_{40}$; blue, $Au_{38/40}$ (scaled with relative abundance).

the curve. The presence of free BINAS (and possibly disulfides) does not strongly interfere with the anisotropy factors at the observed wavelength. If BINAS showed a notable optical activity at 371 nm, it would overrule values for the clusters, because it was used in a 5-fold molar excess.

**Mass Spectrometry of Ligand Exchange Samples and Bidendate Binding.** Mass spectrometry reveals two sets of peaks in the starting material, one corresponding to $Au_{38}$ species, the other one to $Au_{40}$ species (Figure 2A). $Au_{38}/Au_{40}$ nanocluster ligand exchange was monitored with time as shown in Figure 5. The spectra show only partially exchanged species, but there are characteristic differences between $Au_{38}$ and $Au_{40}$ clusters. In the $Au_{38}$ signal set, the original $Au_{38}X_{24}Y_0$ (X, 2-PET; Y, BINAS) is a dominant species, although its relative intensity decreases with time. After 150 h, $Au_{38}X_{24}Y_0$ still constitutes 55% of the $Au_{38}$ signal set. In contrast, the $Au_{40}X_{24}Y_0$ signal disappears completely even after short reaction times (12 h). While a maximum of six 2-PET ligands are exchanged on $Au_{38}$, up to 12 thiol sites ($Au_{40}X_{12}Y_6$) are exchanged in the case of $Au_{40}$ (the signal of maximum intensity is at four BINAS ligands).

BINAS is a dithiol capable of potentially anchoring to two Au atoms, that is, a bidentate ligand. All the ligand exchange samples show that each bidentate BINAS ligand replaces two monodentate $PhCH_2CH_2S$ ligands. This is the first observation of such bidentate ligand coverage in thiolated Au nanoclusters. The average number of BINAS found for the $Au_{38}$ and $Au_{40}$ signal sets and their mixture (scaled with the found ratios between $Au_{38}$ and $Au_{40}$) is shown in Figure 6. Comparison of the curves unambiguously shows that $Au_{40}$ undergoes the ligand exchange much faster and to a higher extent than $Au_{38}$. In $Au_{40}$, the fitted curve (exponential, $R^2 = 0.803$) begins to flatten after 15 h of reaction time, in contrast to $Au_{38}$ ($R^2 = 0.959$), which

saturates only after about 50 h. The overall reaction equilibrates after about 25 h ($R^2 = 0.903$).

In addition to the faster exchange reaction of $Au_{40}$ when compared to $Au_{38}$, the $Au_{38}$:$Au_{40}$ ratio of 88:12 found in the starting material decreases with time and saturates to a ratio of 70:30 after about 20 h. This behavior is in general consistent with the other profiles shown in Figures 4 and 6. The change in the ratio is possibly explained by decomposition of $Au_{38}$ clusters to form insoluble Au−thiolate polymers.[36] Traces of colorless, insoluble materials were observed during the sample processing. The ligand exchange does not lead to size change in the nanocluster core itself as observed in the case of $Au_{25}$.[32]

This suggests two conclusions: (a) $Au_{40}$ is more likely to incorporate BINAS into its ligand shell, and (b) $Au_{38}$ slowly decomposes upon treatment with BINAS. The later is also observed for $Au_{25}(2\text{-PET})_{18}$ clusters.[32] The decomposition of the clusters possibly has structural reasons. The crystal structure of $Au_{25}(2\text{-PET})_{18}$ exhibits six extended $Au_2(SR)_3$ staples.[10] The incorporation of BINAS might lead to steric stress in the ligand or in the staple, because the binaphthyl system is conformationally hindered. Upon exchange, the clusters might decompose to other species that allow the binding of such a ligand. Similar processes might occur in the case of $Au_{38}$.

The "divide and protect" concept and empirical rules allow the prediction of cluster structures to a certain extent.[44] In the case of $Au_{38}$, simulations by Zeng and co-workers predict a fused bi-icosahedral $Au_{23}$ core and nine exterior staples, three short $Au(SR)_2$ and six extended $Au_2(SR)_3$ entities.[45,46]

The simulated minimum geometry of BINAS predicts a sulfur−sulfur distance of ca. 4.1 Å, which is close to the values found for short staples in $Au_{38}$ (ca. 4.7 Å).[47,43] Assuming some flexibility in the staple geometry and the torsion angle of the binaphthyl system, BINAS may provide a suitable structure for the incorporation into short staples. Long staples contain three thiolate ligands. To replace all three positions by BINAS, one has to assume bridging between two staples, because the mass spectra clearly show that one BINAS replaces two (SR) ligands. The observed lack of higher exchange products even at longer times in a large excess of BINAS may suggest that BINAS can easily exchange on short staples but not on the long ones. A systematic variation of ligand concentration and steric properties is warranted and is underway. Shortly after first submission of this Article, the full structure of $Au_{38}(2\text{-PET})_{24}$ was presented.[48] In accordance with our ligand exchange results, the structure in fact bears only three short staples. This strengthens our assumption that BINAS reacts specifically with short staples.

On the basis of this, similar thoughts on the 16e $Au_{40}$ cluster suggest core sizes of 24−28 gold atoms and suitable numbers of staples.[40] Because six BINAS ligands are found in the mass spectrum of $Au_{40}$, we assume a nonspherical structure with 26 core atoms, four extended, and six short staples (Table 1).

**Ligand Exchange with Thiophenol.** The discussed features of the ligand exchange reaction between $Au_{38}/Au_{40}$ and BINAS are based on the bidentate nature of the incoming ligand. To confirm that the slow and incomplete exchange is due to the steric hindrance between long staples and BINAS, we performed exchange reactions with thiophenol (a monodentate thiol) instead of BINAS (sterically hindered bidentate thiol). Thiophenol is monodentate and should therefore not discriminate between the different binding sites of the clusters.

***Table 1.*** Core Atom Numbers and Staple Distributions for $Au_{38}(SR)_{24}$ (Confirmed[46]) and $Au_{40}(SR)_{24}$ (Proposed) Based on Ligand Exchange Results

| | core | (SR)Au(SR) staples | (SR)Au(SR)Au(SR) staples |
|---|---|---|---|
| $Au_{38}(SR)_{24}$ | $Au_{23}$ | 3 | 6 |
| $Au_{40}(SR)_{24}$ | $Au_{26}$ | 6 | 4 |

Ligand exchanges were performed similar to the BINAS case. Briefly, $Au_{38/40}(2\text{-PET})_{24}$ was dissolved in methylene chloride, and a 120-fold molar excess of thiophenol was added (assuming pure $Au_{38}$). The mixture was stirred under inert gas atmosphere at room temperature, and samples at different reaction times were taken. The purification of the clusters was achieved as described in the Experimental Section. Because thiophenol is achiral, no optical activity is expected, and no CD measurements were performed.

Mass spectrometric characterization of the clusters after exchange reveals differences to the exchange with BINAS (see the Supporting Information). After 6 h, the signal for $Au_{38}(2\text{-PET})_{24}$ is no longer the most intense signal in the mass spectra. This is in sharp contrast to exchange with BINAS, where the signal of the starting material remains the most intense signal, even after 150 h. Signals for $Au_{38}(2\text{-PET})_{24-x}(SPh)_x$ with $x = 1-9$ are detectable; this number exceeds the number of ligands bound in short staples in $Au_{38}(SR)_{24}$. As expected, thiophenol exchange also showed an odd number of ligands being incorporated, while BINAS showed only an even number of ligands being exchanged due to the bidentate nature. Similar observations are made for the $Au_{40}$ signal set, where exchange products up to $x = 13$ are detectable. A detailed analysis of the spectra is hard to achieve because the signals for exchanged species overlay with fragment signals and signals for exchanges in the $Au_{40}$ set. A detailed study of ligand exchanges between $Au_{38}$ and monodentate ligands will be presented elsewhere. However, the preliminary results support our assumption that BINAS as a bidentate and conformationally hindered ligand reacts selectively with short staple binding sites in $Au_{38}$ and $Au_{40}$ clusters.

**Relationship between Optical Activity and Ligand Exchange Rate.** The observed optical activity after ligand exchange is strong, and only very few chiral ligands are needed to induce significant optical activity.

The average number of BINAS ligands in the $Au_{38/40}$ set found after equilibration is ca. 1.5. Extrapolation of the corresponding anisotropy factor of ca. $6.5 \times 10^{-4}$ at equilibrium to a full BINAS coverage (12 ligands) leads to anisotropy factors of ca. $5 \times 10^{-3}$. This is higher than the maximum anisotropy factors found for size-separated BINAS-protected clusters (ca. $2 \times 10^{-3}$).[8] It was shown that the optical activity of BINAS-stabilized clusters decreases with increasing cluster size, and the clusters discussed by Gautier et al.[8] are expected to be significantly smaller than $Au_{38}$, because in the applied size exclusion chromatography clusters of masses of $Au_{38}$ cannot be isolated.

In gold nanoclusters, the staple motifs contain an intrinsic stereochemistry that is overall racemic for achiral thiolates. Bridging of an Au adatom between two sulfur atoms transforms

(44) (a) Häkkinen, H.; Walter, M.; Grönbeck, H. *J. Phys. Chem. C* **2006**, *110*, 9927–9931. (b) Chaki, N. K.; Negishi, Y.; Tsunoyama, H.; Shishibu, Y.; Tsukuda, T. *J. Am. Chem. Soc.* **2008**, *130*, 8608–8610.
(45) Pei, Y.; Gao, Y.; Zeng, X. C. *J. Am. Chem. Soc.* **2008**, *130*, 7830–7832.
(46) Lopez-Acevedo, O.; Tsunoyama, H.; Tsukuda, T.; Häkkinen, H.; Aikens, C. M. *J. Am. Chem. Soc.* **2010**, *132*, 8210–8218.
(47) Gautier, C.; Bürgi, T. *J. Phys. Chem. C* **2010**, *114*, 15897–15902.
(48) Qian, H.; Eckenhoff, W. T.; Zhu, Y.; Pintauer, T.; Jin, R. *J. Am. Chem. Soc.* **2010**, *132*, 8280–8281.

the sulfur atoms into stereocenters, because they are ligated by a surface gold atom, the adatom, the ligands' organic backbone, and a lone pair.[49] The cis and trans configurations in short staples are diastereomeric and should differ in their physical properties (for long staples, the situation is more complex but in principle the same ideas apply). Introduction of BINAS into these staples might induce preferred configurations to other staples in its surrounding. This might enhance the asymmetry of the overall cluster. Besides, the crystal structure of $Au_{38}$ shows an interesting feature: the arrangement of the short staples on the cluster surface is asymmetric, making the whole molecule intrinsically chiral.[46] Both enantiomers are found in the unit cell of the crystal. Similar argument holds true for $Au_{102}$ clusters.[16] Therefore, an enrichment of one of the enantiomers of $Au_{38}$ itself under the induction of an enantiopure ligand (BINAS) is plausible. This requires certain flexibility for rearrangement of the whole cluster.

Altogether, different levels of chirality have to be considered: (a) the trivial case of protection of the cluster with an enantiopure ligand; (b) distribution of cis and trans geometries of staples (and more complicated for longer staples); and (c) the intrinsic chirality of the cluster achieved by the arrangement of the ligands on the cluster surface. These recent experimental crystal structures of gold nanoclusters shed new light on the optical activity of such systems. Cooperation of these effects might explain the relatively strong optical activity.

## Conclusion

The ligand exchange on $Au_{38}(2\text{-PET})_{24}$ and on $Au_{40}(2\text{-PET})_{24}$ with bidentate BINAS is incomplete. The kinetics of the exchange reaction slows drastically after few hours even in a huge excess (2-PET:BINAS 1:5) of BINAS. We suggest structural reasons such as the number of short staple motifs being limiting factors in the exchange reaction, in contrast to exchange reactions with monodentate ligands, which are nearly complete.[35] This assumption is supported by the decomposition of $Au_{25}$ clusters in a similar reaction as the crystal structure of $Au_{25}$ reveals only extended staples that are not likely to incorporate BINAS. In $Au_{40}$, the exchange was found to be more favored and faster than in $Au_{38}$. This suggests a greater number of short staples in $Au_{40}$ clusters, and we assume an $Au_{26}$ core for $Au_{40}(SR)_{24}$ and an $Au_{23}$ core for $Au_{38}(SR)_{24}$ clusters, as confirmed by its crystal structure. On the basis of MS data, the overall exchange of suitable ligands in short staples by BINAS is about 20% for $Au_{38}$ (three short staples) and about 60% in $Au_{40}$ (six short staples) clusters.

Mass spectrometry shows that BINAS replaces two (2-PET) ligands on the clusters, which indicates that singly bound BINAS is very unlikely. Over the course of the reaction time, the ratio between $Au_{38}$ and $Au_{40}$ varied, which is possibly due to decomposition to form Au(I)−thiolate polymers, as a colorless material was observed during the workup of some samples. It is suggested that the bidentate nature of BINAS is responsible for the incomplete reaction as the binding sites in gold nanoclusters are chemically different and steric reasons might play a key role. In future work, BINAS or other suitable bidentate ligands might be used as sensors for the number of short staples in gold nanoclusters.

The limited exchange rates (up to 6 and 12 binding sites, respectively) are due to the bidentate BINAS ligand. This is demonstrated by performing similar experiments with monodentate thiophenol. In this case, the exchange is much faster, and more binding sites are exchanged. This indicates sensitivity of BINAS toward the number of short staples in the clusters.

The reaction was monitored with CD spectroscopy, and a strong optical activity was found to be imparted on the clusters. A red-shift in the onset of optical activity as compared to the CD spectrum of free BINAS gives evidence for successful ligand exchange, as was confirmed by MS. Significant optical activity is found after only 15 min of reaction time. The increase in optical activity begins to saturate after 20 h and shows a maximum anisotropy factor at 150 h of $6.6 \times 10^{-4}$. The observed significant optical activity at very short reaction times is surprising in view of the small amount of ligand exchanged. We assume induction of preferred cis/trans configurations in the staples by introduction of BINAS and enhancement of the asymmetry of the whole cluster as well as enrichment of one of the enantiomers of $Au_{38}$ itself.

The combination of CD spectroscopy and mass spectrometry to observe ligand exchange reactions is shown to be a powerful combination to gain insights into the time scales of such reactions. In situ circular dichroism spectroscopy is a quick and invasion-free tool to get information about the time scale of equilibration. These results are confirmed by purified samples, indicating minor/almost no contribution of free ligands to the optical activity. Mass spectrometry provides information about both cluster sizes and ligand shell composition. Preliminary results to explain the relationship between nanocluster properties and ligand distribution in mixed-shell thiolate protected gold nanoclusters are presented.

**Acknowledgment.** We thank Prof. S. Gladiali (Università di Sassari, Sassari, Italy) for the synthesis and donation of the enantiopure BINAS used in this work. Dr. Matthias Mayer (University of Heidelberg) is gratefully acknowledged for providing the CD spectrometer. Also, we thank Dr. Cyrille Gautier (Metalor Technologies International SA, Neuchâtel, Switzerland) for providing CD spectra of BINAS and BINAS cyclic disulfide. A.D. gratefully acknowledges support from the National Science Foundation (NSF 0903787). We also acknowledge the reviewers' comments.

**Supporting Information Available:** Additional CD spectra and anisotropy factor curves and mass spectra. This material is available free of charge via the Internet at http://pubs.acs.org.

JA104641X

(49) Vozzny, O.; Dubowski, J. J.; Yates, J. T., Jr.; Maksymovych, P. *J. Am. Chem. Soc.* **2009**, *131*, 12989.